STUDY OF DRUG-DNA INTERACTION USING QUANTUM MECHANICAL TOOLS

SUMMARY

THESIS SUBMITTED FOR THE AWARD OF THE DEGREE OF

Doctor of Philosophy

in

Applied Physics

By

Ruchi Mishra

Enrolment No.: 266/13

Under the Supervision of

Dr. Ramesh Chandra

BABASAHEB BHIMRAO AMBEDKAR UNIVERSITY
LUCKNOW
प्रज्ञा शील करुणा
ESTABLISHED 1996

Department of Applied Physics
School for Physical Sciences
BabasahebBhimraoAmbedkar University, Lucknow-226025
U.P. (India)

2018

STUDY OF DRUG-DNA INTERACTION USING QUANTUM MECHANICAL TOOLS

Chapter 1: Introduction

DNA is the pharmacological target of many anticancer drugs which are currently under clinical trials. Transcription and replication are the vital processes essential for the survival of the living systems. In transcription, information is fetched from DNA to RNA and has recourse to synthesize protein in the body. In replication, DNA yield self-replication process and reconstruct two identical strands. DNA starts these processes only after receiving the signal which is usually in the form of regulatory protein to a specific region of DNA. If this regulatory protein is mimicked by a drug molecule (mainly heterocyclic aromatic molecule), then the functions of DNA can be artificially modulated, inhibited or activated by this small molecule to cure or control a disease.

DNA plays an extremely important role for drug action, for many biological activities (anti-tumor, antiviral and antimicrobial) because many compounds have ability to bind with DNA sequence specifically and interfere with DNA topoisomerases or with transcription factor. The activity of some drugs for the treatment of cancer, genetic disorders, and other viral diseases depend upon their binding mode with DNA or modification of DNA activity. The study of interaction of drug with DNA is very interesting and efficient not only to learn the mechanism of interactions but also for designing new drugs. Although the mechanism of drug- DNA interaction is not known in detail. It is necessary to explore more simple methods for investigating their interaction mechanism. The current research effort focuses on the computational methods which are

used to investigate the molecular basis for drug-DNA recognition, the role of water in mediating weak interaction. Thus, the investigation of drug-DNA interaction could be helpful to discover new and advanced drug candidates.

There are two key modes in which drug molecules can interact with DNA such as surface binding to their minor or major grooves, intercalation between adjacent base pairs. Both covalent as well as non-covalent interactions were found between drug molecules and DNA. Covalent binding in DNA is irretrievable and regularly points to complete inhibition of DNA processes and subsequent cell death. Drug molecule covalently binds with DNA via inter- and intra-strand cross linking or alkylation. Covalent binders of DNA have high binding strength. The covalent binders are also known as alkylating agents because they can attach an alkyl group to DNA and are also used in the treatment of Cancer. Non-covalently binding of drug with DNA is mainly classified into two category viz. groove binders and intercalators. Groove binders are of two types: minor groove binders and major groove binders. Groove binders are highly sequence-specific. The two types of grooves in nucleic acid differ in hydrogen-bonding, electrostatic potential and in degree of hydration. Mainly the large protein molecules bind to the major groove of DNA while small molecules generally bind to the minor groove of DNA which are long elongnated structures with a curvature that accompaniment the shape of the minor groove. Another type of non-covalently binding drugs is intercalators which are generally planar heterocyclic molecule which stacks between the two adjacent nucleic acid base pairs. The complex remains stabilized because of π-π stacking between the drug molecule and DNA bases.

The drug-DNA interaction can be explained by experimental and molecular modelling studies. UV-visible, fluorescence spectroscopies, Circular dichorism, Viscosity measurements, Thermal denutration studies and cyclic voltammetry are the commonly used experimental techniques that have been used as a primary tool to characterize the behavior of drug-DNA binding and the consequences of such type interaction on the structure of nucleic acid. Molecular modelling methods are able to identify and define key details of molecular interaction using high quality molecular graphics tools. Computer modelling has risen as a powerful tool for experimental and theoretical investigations. Visualization of experimental data in a 3D, atomic-scale model cannot just clarify startling outcomes yet regularly brings up new issues, which influences future research. Molecular Docking, Molecular Dynamics simulations, MMPBSA/MMGBSA, QSAR, Virtual Screening and QM/MM are the important molecular methods which can be used to explore the binding of drug with DNA.

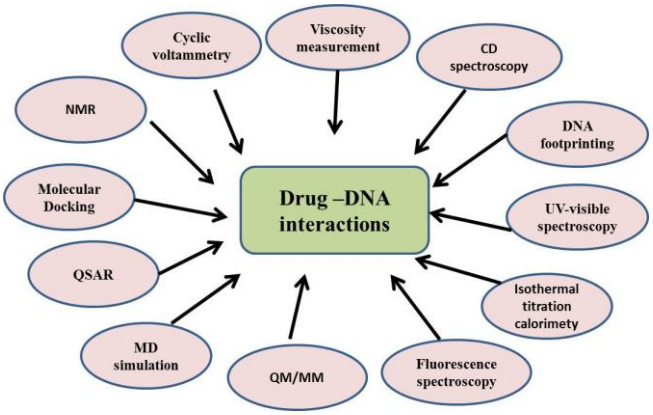

Fig. 1: Different types of experimental and theoretical methods used to study drug-DNA interaction.

Chapter 2: Methodology

Geometry optimization of studied drug molecules has been carried out using Gaussian 09 at B3LYP/6-31G* level. After geometry optimization molecular docking was performed using AUTODOCK and the best pose was analyzed. MD simulations of the selected docked poses were performed using GROMACS or AMBER. In MD simulation, the complex is put into the water box and relaxed by a series of constrained energy minimization and MM runs at the MM level. After equilibration the system is subjected to a classical MD production runs and the binding energy between drug and DNA was calculated using MMPBSA/MMGBSA method. Snapshots obtained from the MD simulation are taken as starting geometries for the QM/MM calculations. The QM/MM calculations were performed with two-level ONIOM method within the Gaussian 09 program suite (Fig. 2). DFT method along with basis set 6-31+G (d, p) is used for the high layer and AMBER force field for the low layer and all the water molecules are freezed. Geometry optimization of above system was performed and the energy of the high or QM region is calculated. Now, the co-ordinate of QM region from the above optimized system is extracted, which further subjected for geometry optimization and the single point energy calculations of QM region in gas phase using same method. The interaction energy between the DNA and drug molecule is calculated with the help of formula-

$$\Delta E_{I.E} = E_{QM(g,p)} - E_{QM(p,p)} \quad (1)$$

where, $\Delta E_{I.E}$ is the interaction energy between drug and DNA. E_{QM} (p, p) is the energy of QM region in protein phase and E_{QM} (g, p) is the energy of QM region in gas phase.

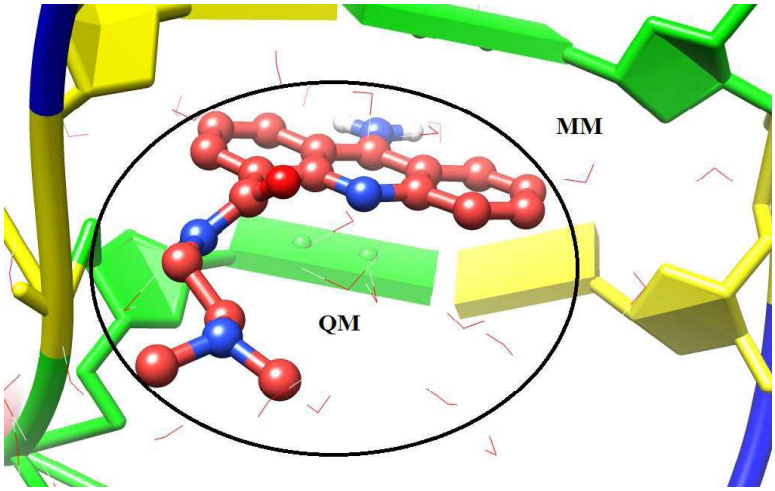

Fig. 2: Two Layered ONIOM Scheme.

Chapter 3: Molecular Docking and Molecular Dynamics Study of DNA Minor Groove Binders

In this chapter, two major DNA minor groove binders classes, polyamides and diarylamidines are undertaken for the study. The crystal data of the B-DNA (1D30, 195D, 1D86 and102D) were downloaded from the Protein Data Bank. The drug molecules extracted from these complexes were subjected to geometry optimization using Gaussian 09 at B3LYP/6-31G* level. Molecular docking calculations were performed using AUTODOCK. It is revealed that all the ligands bind to AT-rich region of DNA with good docking fitness score. Comparison between experimental and calculated binding energies obtained from docking studies shows that the complex having lowest experimental binding energy also has the lowest calculated binding energy and vice-versa. This shows the ability of AUTODOCK in predicting the correct binding modes for drug DNA complex. MD simulation from AMBER15 and GROMACS 4.5.6 were performed for the best poses selected from the docking studies. RMSD as a function of time is plotted for all the complexes to obtain the

systematic deviation of complexes and convergence of RMSD shows the stability of the complexes. The binding energies were calculated using the "mm_pbsa.pl" script implemented in AMBER and g_mmpbsa method in GROMACS. It has been observed that the energies calculated using g_mmpbsa and the AMBER MMPBSA package are approximately similar and the difference of 1-3 kcal/mol has been observed due to the difference in ΔG_{polar} (Table 1). The difference in ΔG_{polar} observed because of different algorithms, implemented in APBS and PBSA.

Table 1: Comparison of binding energy components obtained from AMBER MMPBSA and g_mmpbsa.

PDB Id	Program	ΔE_{elec} [a]	ΔE_{vdw} [b]	ΔG_{polar} [c]	$\Delta G_{nonpolar}$ [d]	$\Delta G_{binding}$ [e]
1D30	mm_pbsa.pl	-25.80±6.54	-34.83±3.39	39.27±6.40	-4.15±0.22	-25.52±3.64
	g_mmpbsa	-12.01±5.18	-16.42±7.24	17.84±7.12	-1.71±0.58	-25.95±10.11
1D86	mm_pbsa.pl	-51.80±13.59	-30.43±4.80	65.35±12.44	-4.10±0.33	-20.98±6.58
	g_mmpbsa	-17.60±12.47	-27.36±12.61	25.41±14.16	-2.92±1.16	-22.46±13.18
102D	mm_pbsa.pl	-32.25±10.30	-22.56±3.63	41.63±8.77	-3.76±0.20	-16.94±4.06
	g_mmpbsa	-11.91±4.10	-26.51±5.13	20.65±5.75	-2.89±0.41	-20.66±7.33
195D	mm_pbsa.pl	-26.25±14.81	-27.46±3.69	39.99±14.48	-3.93±0.39	-17.65±4.36
	g_mmpbsa	-26.26±4.31	-34.99±3.61	37.72±6.65	-3.75±0.27	-27.30±4.17

[a]Electrostatic component to the binding energy in kcal/mol.

[b]van der Waals component to the binding energy in kcal/mol.

[c]Polar solvation energy in kcal/mol.

[d]Non-polar solvation energy in kcal/mol.

[e]Binding energy in kcal/mol.

The analysis from the root mean square deviation for the stability of complex shows that the AMBER force fields are better for the drug-DNA complexes up to 5ns of molecular

dynamics simulations. However, longer simulations may give a more detailed view of the difference in the force fields. This analysis can be helpful for the improvement of existing minor groove binders, and also in designing novel chemical entities which can act as a good DNA inhibitor.

Chapter 4: Illustrating Binding Mechanism of DNA intercalators using Computational Approaches

In the present chapter, the interaction studies on DNA intercalators, DACA, AAC, mitoxantrone, emodin and benzidine have been performed with the nucleic acid using various molecular modelling approaches. The experimental binding constant of these compounds with DNA has been collected from the literature. From the docking studies, it was found that all the drug molecules intercalate between the G-C pairs of DNA. The docked poses are stabilized by π–π stacking and by the formation of hydrogen-bonds between the DNA base pairs and functional group (Fig 3).

Table 2: Comparison of experimental and calculated ΔG_{bind} obtained from molecular docking studies and MMPBSA/MMGBSA calculations using AMBER and GROMACS.

Ligand	**No. of heavy Atoms in Ligand**	**Exp. ΔG_{bind}**	**Calc. ΔG_{bind} (Docking)**	**Calc. ΔG_{bind} (MD)**		
				GROMACS	**AMBER**	
				MMPBSA	**MMPBSA**	**MMGBSA**
Mitoxantrone	32	-7.64	-6.86	-46.66±4.36	-32.39±2.86	-27.25±2.30
AAC	23	-7.68	-7.72	-38.67±3.16	-29.07±2.55	-32.73±3.23
DACA	22	-8.03	-7.99	-35.80±3.63	-30.54±2.64	-31.55±2.59
Emodin	20	-5.12	-6.90	-35.18±2.55	-25.85±2.99	-24.35±2.36
Benzidine	14	-4.26	-5.51	-19.12±4.96	-16.51±2.61	-17.61±2.94

All the energies in kcal/mol.

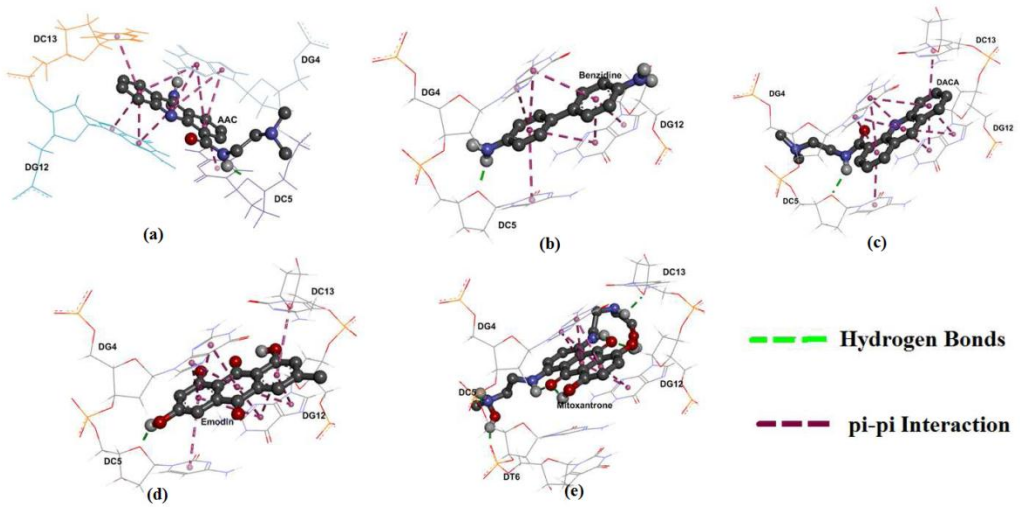

Fig. 3: Different types of non-covalent interactions obtained from Molecular Docking. Hydrogen bonds are indicated by dotted lines and π–π interactions by purple dotted lines for the ligand (a) AAC (b) Benzidine (c) DACA (d) Emodin (e) Mitoxantrone.

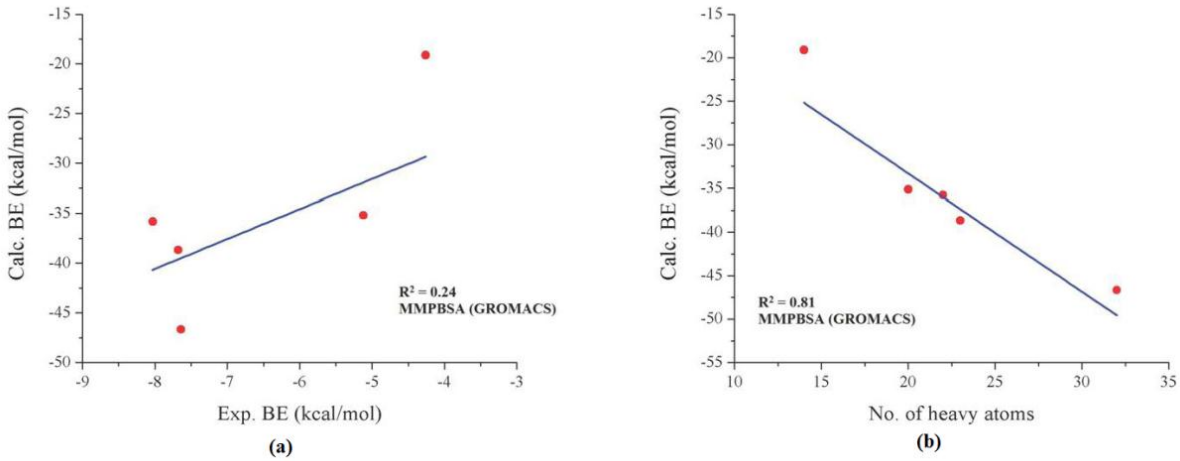

Fig. 4: Variation of calculated binding energy obtained from (a) MMPBSA (b) MMGBSA calculations using AMBER with experimental binding energy.

The plot between experimental binding energy and calculated binding energy values shows a linear correlation (R^2 = 0.24). The plot between the number of heavy atoms versus calculated binding energy also has a linear correlation (R^2 = 0.81), and indicates

that with the increase in the size of the drug, the binding energy of drug-DNA complexes also increases (Fig. 4). In the case of AMBER, the binding energy values were calculated using MMPBSA and MMGBSA method which shows a good correlation with experimental values with R^2 = 0.78 for MMPBSA and R^2 = 0.75 for MMGBSA method (Fig. 5).

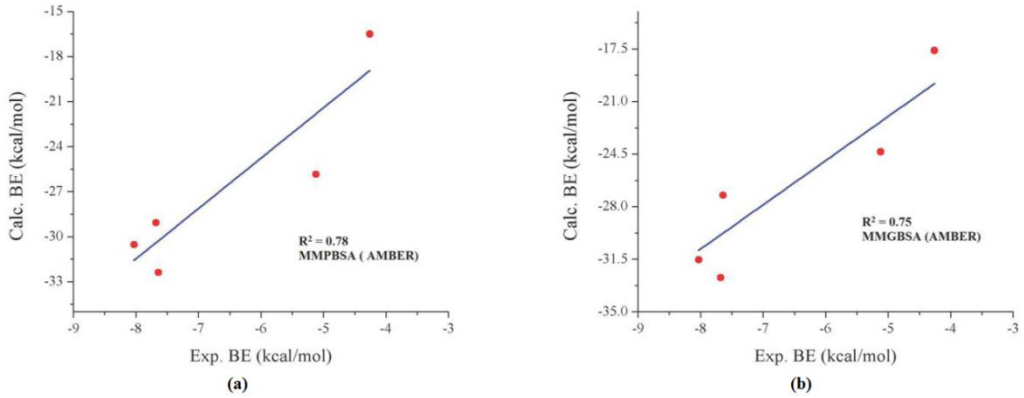

Fig. 5: Variation of calculated binding energy obtained from (a) MMPBSA (b) MMGBSA calculations using AMBER with experimental binding energy.

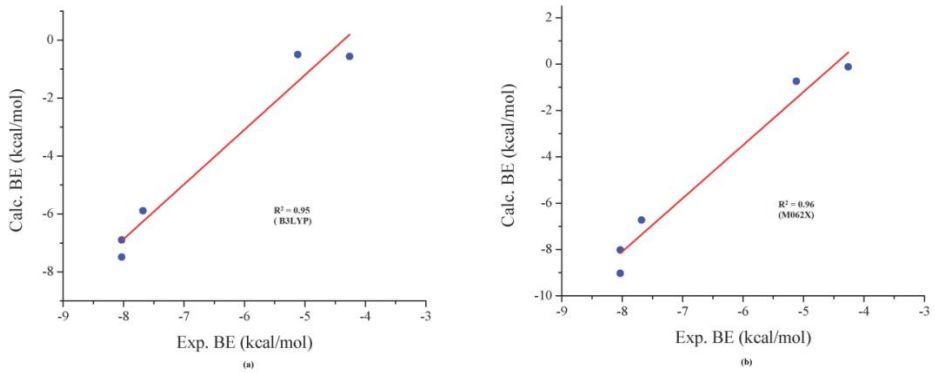

Fig. 6: Variation of calculated binding energy with experimental binding energy from QM/MM calculations using (a) B3LYP (R^2 = 0.95) (b) M062X (R^2 = 0.96) as a basis set for the QM region (GROMACS).

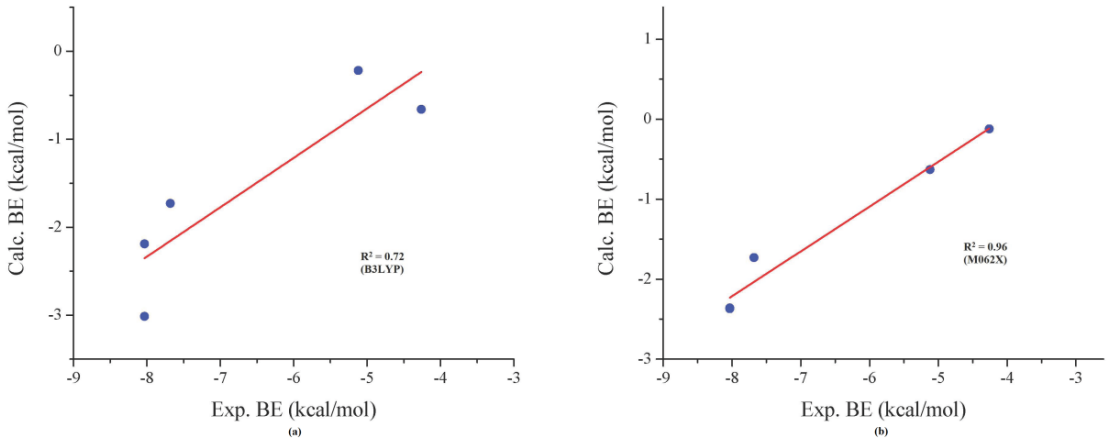

Fig. 7: Variation of calculated binding energy with experimental binding energy from QM/MM calculations using (a) B3LYP (R^2 = 0.72) (b) M062X (R^2 = 0.96) as a basis set for the QM region (AMBER).

The experimental binding energy values shows good correlation with calculated binding energy values obtained from the QM/MM calculations (GROMACS snapshots) for both method i.e. B3LYP (R^2 = 0.95) and M062X (R^2 = 0.96) as shown in Fig. 6. The correlation plot between calculated binding energy from the QM/MM calculations (from AMBER snapshots) and experimental binding energy shows a good linear correlation with correlation coefficient R^2 = 0.72 for the B3LYP and R^2 = 0.96 for M062X shown in Fig. 7.

From the above results and figures, it is clear that the binding energy values obtained from the QM/MM calculations complements more with experimental data than that of the molecular docking calculations and MMPBSA calculations. Therefore, QM/MM study provides better insight on the complexity in binding modes of small molecules to DNA.

Chapter 5: The role of Quantum Mechanics/Molecular Mechanics calculations in understanding the binding of DNA minor groove binders

In this chapter the recognition of 13 DNA-minor groove binders complexes in sequence-selective manner are presented by *in silico* methods, which provides the basis for designing new drugs. The crystal data of the drug-DNA complexes were downloaded from the Protein Data Bank with PDB Id 127D, 2D64, 1D30, 1D64, 1D63, 121D, 102D, 109D, 195D, 1D86, 2DBE, 1PRP, 227D and their experimental binding energies were collected from literature. The water molecules and the ligands were removed and the crystal structure of B-DNA was extracted from their respective drug-DNA complex crystal structure. The drug molecules extracted from these complexes were subjected to geometry optimization using Gaussian 09 at B3LYP/6-31G* level. The chemical structure of minor groove binders which were used for the further study is shown in Fig. 8.

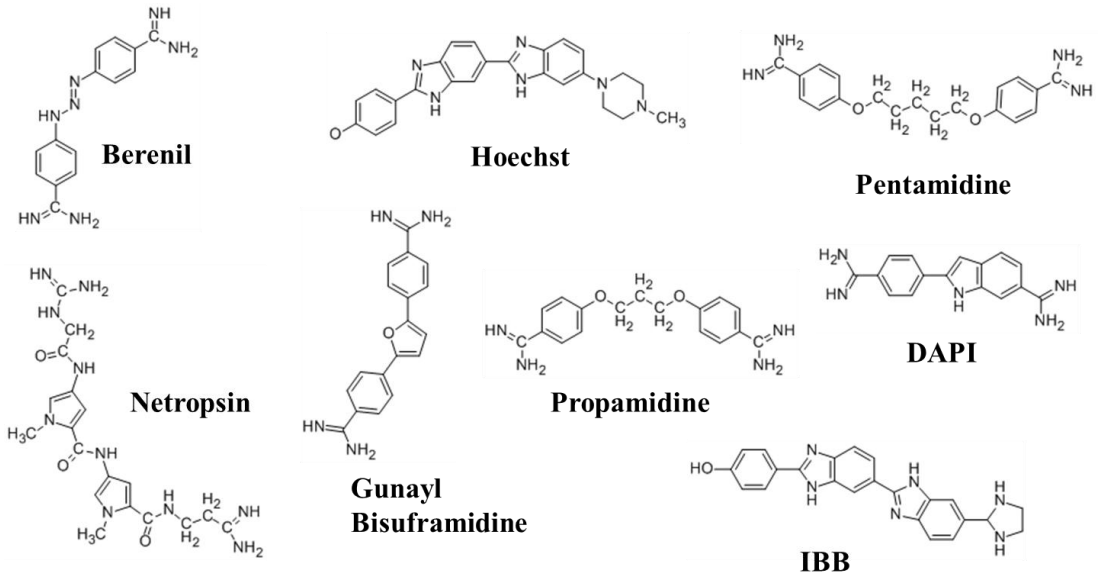

Fig. 8: Chemical Structure of Minor Groove Binders.

Docking studies reveal that the ligands are stacked in the minor groove of DNA duplex via van der Waal and hydrophobic interactions. Additionally, the minor groove binding drugs exhibit strong hydrogen bonding to the nucleic acid bases. From the results, this is concluded that the minor groove binders generally bind to the A and T DNA residues (Fig. 9). The calculated binding energy obtained from molecular docking (Table 3) linearly correlates to the experimental with R^2=0.87.

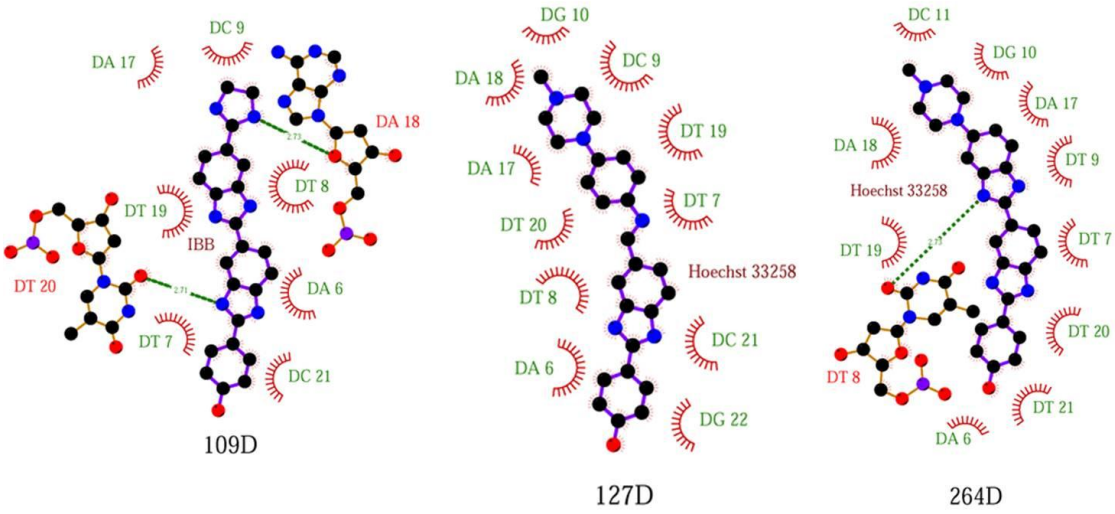

Fig. 9: Different types of interactions obtained from molecular docking studies for top three stable complexes.

The average RMSD values for the DNA-Ligand complexes and free DNA is 0.2-0.3 nm and ligands within the last 3ns of the simulations are 0.2-0.3 nm and 0.03-0.1 nm respectively, while the average RMSD of free ligands are 0.03-0.1 nm except for PDB Id 195D. The RMSD profile of all the systems indicates the result of dynamic behavior of DNA-Ligand complexes from the initial position to final position throughout the simulation time (Fig. 10).

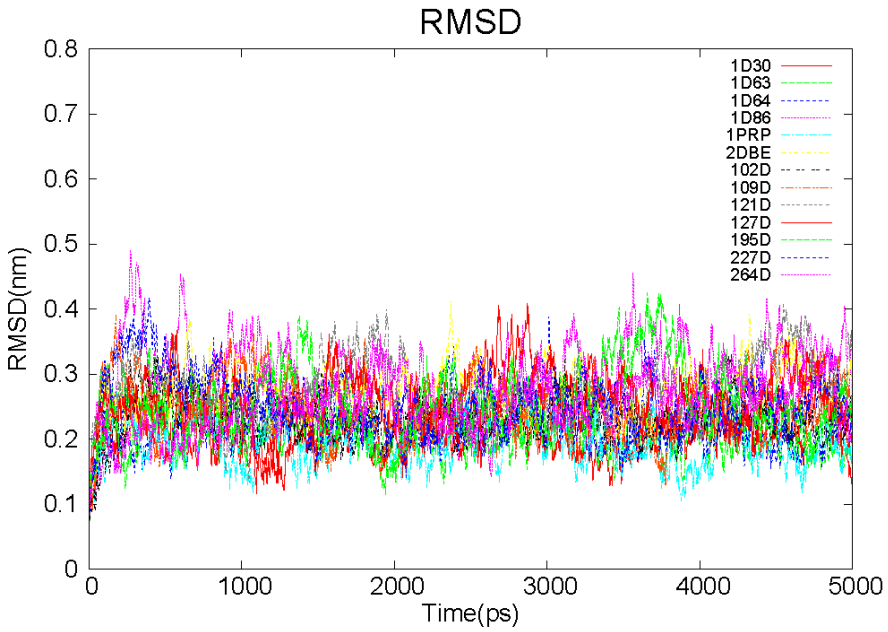

Fig. 10: RMSD profile for DNA-Ligand complexes.

The MMPBSA calculations were performed to calculate the strength of interaction between ligand and DNA, which can be measured by the binding energy values presented in Table 3. Fig. 11 shows the binding energy contributions of residues for all DNA-ligand complexes. Fig. 12 shows the contribution of each component of energy to the final binding energy and it was analyzed that the contribution of van der Waals interaction is greater than that of electrostatic energy to the final binding energy.

Interaction energies at each nanosecond were calculated using ONIOM scheme by employing two different methods B3LYP and M062X. The geometry optimization was performed using the basis set 6-31G* for the QM region and Amber force field for MM region. The calculated interaction energies from QM/MM calculation shows good correlation with experimental binding energies at 1ns snapshots from both B3LYP and M062X method for QM (Fig. 13).

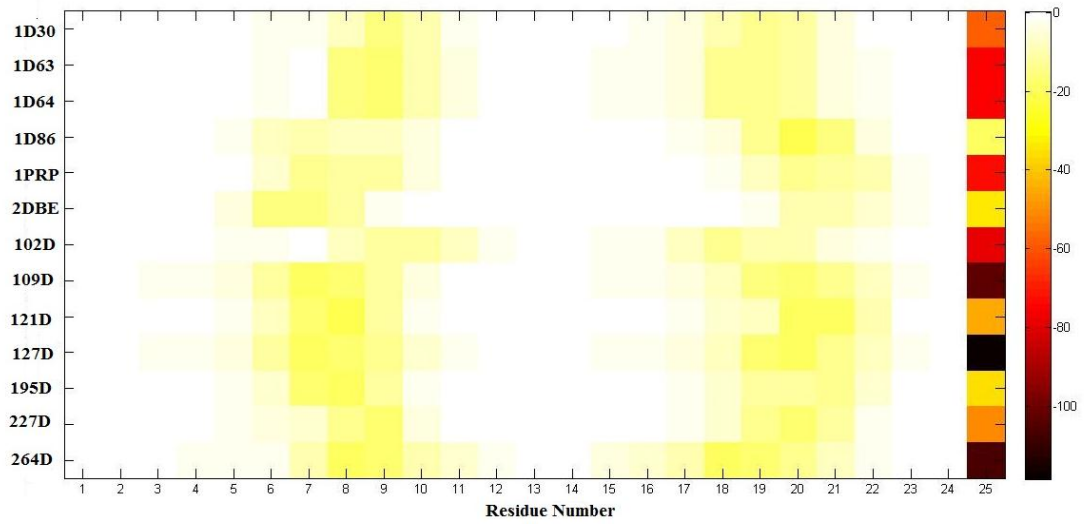

Fig. 11: Energetic contribution of DNA residues in the binding in kilojoules/mol.

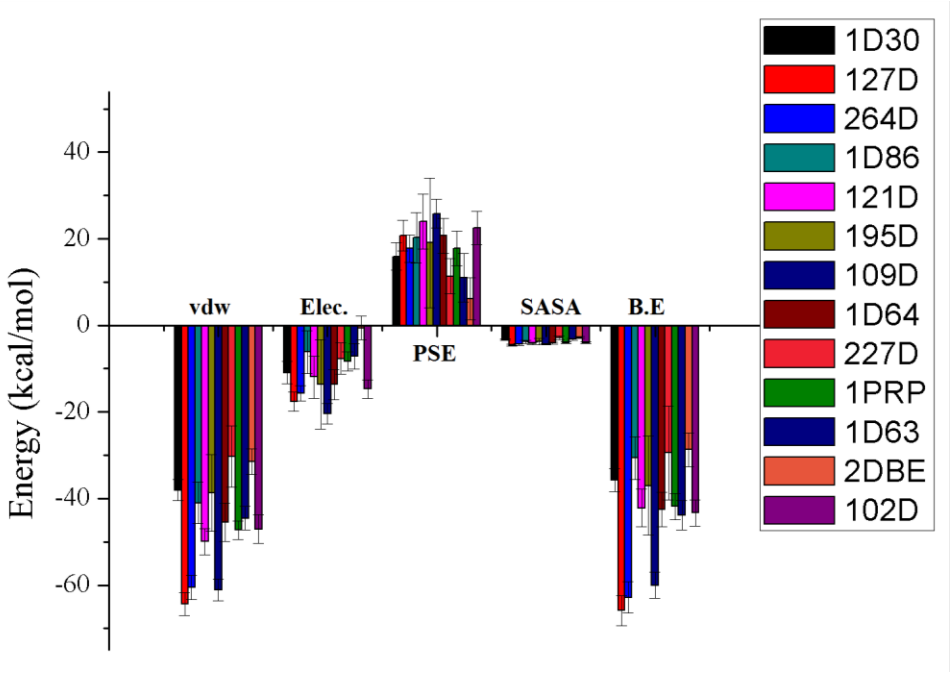

Fig. 12: Histogram depicting view of the contribution of each and every component of energy to the final binding energy.

Table 3: Interaction energies of DNA-Ligand complexes at various time scales and comparison with experimental binding energy (ΔG_{bind}).

PDB Id	Exp. BE	IE					
		0-1ns	**1-2ns**	**2-3ns**	**3-4ns**	**4-5ns**	**0-5ns**
127D	-11.0	-63.41±3.22	-65.25±2.93	-66.16±2.83	-68.43±2.95	-64.65±2.87	-65.83±3.42
264D	-11.7	-61.48±3.47	-63.93±3.31	-61.70±3.12	-63.66±3.58	-61.76±3.51	-62.75±3.58
1D86	-8.8	-32.10±6.16	-30.74±3.58	-31.95±4.74	-28.25±4.24	-29.46±4.15	-30.62±4.90
121D	-8.6	-42.79±3.45	-40.55±3.67	-40.55±4.04	-44.05±4.20	-41.88±5.01	-42.17±4.35
195D	-8.7	-38.27±4.33	-39.24±5.65	-37.38±6.42	-34.27±4.24	-35.90±4.82	-37.01±5.45
109D	-12.0	-58.04±3.12	-60.64±2.73	-60.65±2.78	-60.45±2.46	-58.75±2.67	-59.90±2.98
1D64	-7.0	-41.73±3.13	-41.96±3.65	-39.01±3.59	-43.02±3.63	-45.80±2.76	-42.51±4.04
227D	-9.3	-35.68±3.34	-36.16±4.68	-38.16±3.11	-39.99±2.99	-39.36±3.24	-37.87±3.91
1PRP	-8.2	-39.58±2.78	-41.57±2.71	-43.41±2.67	-43.41±2.67	-41.28±2.81	-41.80±3.05
1D30	-8.0	-36.82±2.38	-35.60±3.01	-34.71±2.24	-35.75±2.50	-35.10±2.44	-35.76±2.64
1D63	-8.0	-42.85±3.32	-42.29±2.87	-44.64±3.00	-44.10±4.02	-44.21±2.96	-43.75±3.39
2DBE	-8.6	-28.22±3.43	-29.17±3.57	-27.55±5.38	-31.20±4.07	-26.30±3.26	-28.74±3.98
102D	-8.2	-42.75±2.85	-45.24±2.69	-43.85±2.64	-41.99±2.70	-41.52±2.62	-43.28±3.03

All the energy values are in kcal/mol.

It was observed that the interaction energy of DNA-Ligand complexes does not only depend on the chemical structure of ligand but also depends on the DNA sequence and specificity. The different interaction energies were observed in the interaction of Hoechst with two different DNA sequences, this is due to difference in the DNA sequences and similarly for the case of Netropsin, Berenil and propamidine.

A computational approach that combines with quantum mechanics, molecular docking, and molecular dynamics simulation predict the energetic pattern of the DNA-Ligand binding. Molecular Docking helps to predict the perfect binding pockets and MD

simulation results highly support the predicted binding site. QM/MM calculations also predict the similar binding mode predicted from Docking and Molecular dynamics.

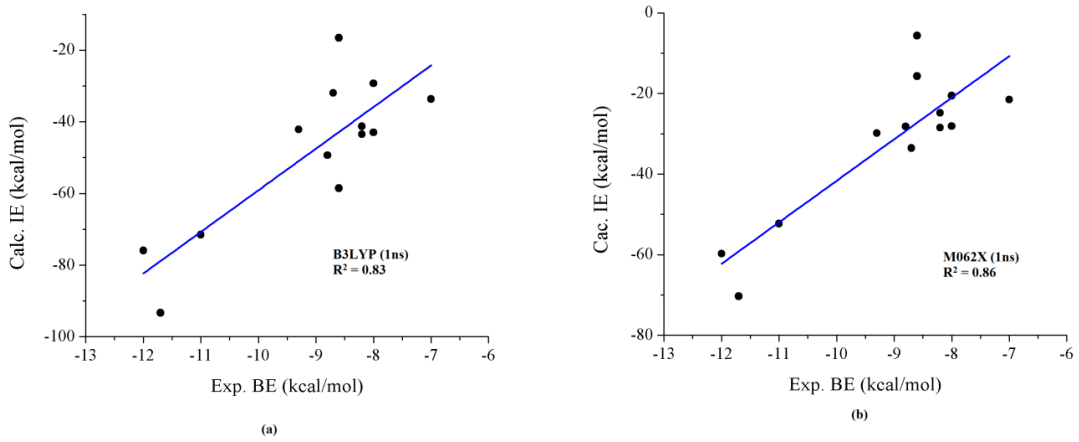

Fig. 13: Variation of interaction energy with experimental binding energy from QM/MM calculation using (a) B3LYP (b) M062X method for QM region.

Chapter 6: Cross Molecular Docking and Molecular Dynamics Studies of DNA Binding Ligands

Large number of biological structures in databases is increasing rapidly; molecular docking is a popular approach to deal with conformation or even to explain the interaction between potential drug molecules and their biomolecular targets. Mostly all the scoring functions are parameterized for protein-ligand complexes and docking programs are validated for protein-ligand docking. The structural features of nucleic acid is unique such as high density charge and helix chiral geometry and nucleic acid do not have any predefined binding site which is present in proteins. This leads to a question

whether the docking programs which are applicable for the protein-ligand docking can also reproduce results for nucleic acid-ligand or not.

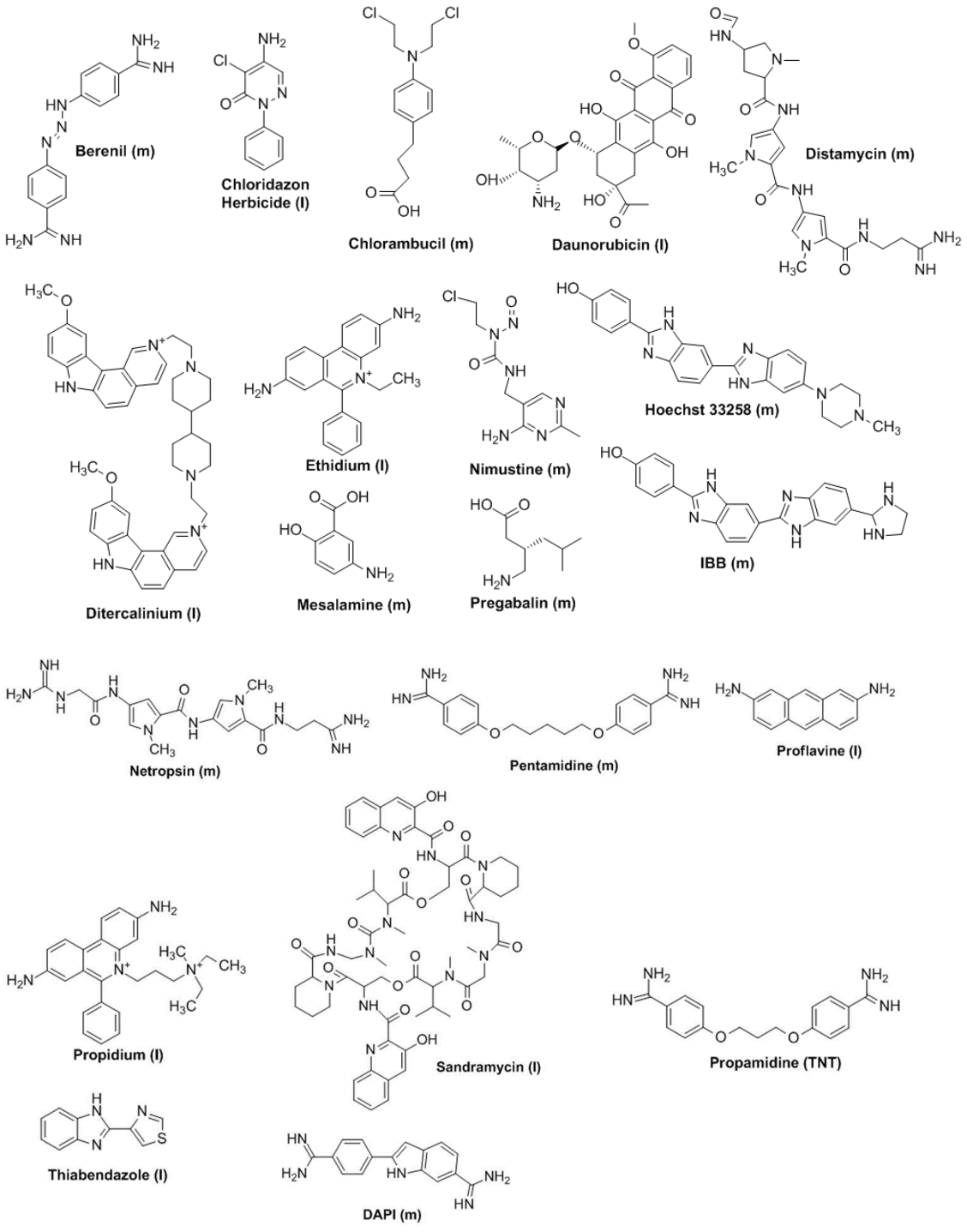

Fig. 14: Chemical Structure of DNA binding Ligands with their binding mode.

The critical issue arises when the binding mode of ligand is unknown to the DNA and there is no previous experimental data available, and then it is difficult to select which oligomer conformation should be used as target. It is observed that if the target DNA has an artificial intercalation gap, then the docking is able to predict the correct binding mode which is energetically most favorable; which suggests that the AutoDock score function is efficient to evaluate ligand-DNA interactions at least in a qualitative way. In the present study some of the DNA binding ligands which are known intercalator or minor groove binders (Fig. 14) are used and the two DNA sequences are taken, 1) with intercalation gap (PDB Id 2DES) ; 2) without intercalation gap (PDB Id 1BNA).

Table 4: Comparison of experimental and calculated ΔG_{bind} (kcal/mol) obtained from molecular docking studies and MMPBSA calculations using GROMACS.

Ligand	**Exp. B.E.**	**Docking**		**MMPBSA**	
		6mer	**12mer**	**6mer**	**12mer**
Berenil (m)	-8.0	-6.82 (m)	-8.57 (m)	-28.33±3.84	-35.55±3.11
Chloridazon Herbicide (I)	-5.91	-6.08 (m)	-7.14 (m)	-24.86±3.09	-25.37±3.03
Cholrambucil (m)	-4.26	-3.67 (m)	-6.04 (m)	-25.66±4.51	-23.28±5.58
Daunorubicin (I)	-7.9	-9.26 (I)	-11.07 (m)	-55.28±4.8	-35.42±10.92
Ditercalinium (I)	-11.9	-11.68 (I)	-13.21 (m)	-338.52±7.17	-469.15±7.03
Distamycin (m)	-10.5	-5.82 (m)	-8.4 (m)	-24.17±10.37	-24.25±8.11
Ethidium (I)	-6.7	-7.28 (I)	-8.23 (m)	-190.82±3.58	-242.81±3.57
Hoechst (m/I)	-11.7	-9.34 (m)	-13.93 (m)	-16.41±9.62	-43.51±7.71
IBB (m)	-12.0	-10.04 (m)	-14.59 (m)	-50.34±7.05	-54.20±9.86
Mesalamine (m)	-4.2	-3.77 (m)	-5.4 (m)	-18.59±5.61	-21.17±2.44
Nimustein (m)	-4.8	-5.8 (m)	-7.39 (m)	-24.14±3.76	-19.73±7.03
Netropsin (m)	-8.7	-6.85 (m)	-8.35 (m)	-31.91±4.92	-36.92±7.18
Pentamidine (m)	-7.0	-5.84 (m)	-8.23 (m)	-22.91±6.10	-41.31±3.76
Pregabalin (m)	-6.5	-4.76 (m)	-5.22 (m)	-5.80±10.29	-14.13±3.15
Proflavin (I)	-8.7	-6.31 (I)	-8.22 (m)	-182.71±3.21	-241.90±2.63
Propidium (I)	-7.5	-7.29 (I)	-7.72 (m)	-30.66±5.40	-29.01±6.57
Sandramycin (I)	-10.3	-9.34 (I)	-6.52 (m)	-43.30±3.2	-40.05±8.09
Thiabendazole (I)	-5.2	-5.4 (m)	-7.61 (m)	-4.46±9.00	-28.29±7.78
Propamidine (m)	-7.0	-6.5 (m)	-9.22 (m)	-35.08±5.93	-46.10±3.84
DAPI(m)	-8.0	-6.86 (m)	-9.55 (m)	-29.59±5.19	-39.83±2.23

All the energies are in kcal/mol.

Molecular modelling studies such as molecular docking, MD simulation, MMPBSA and MMGBSA calculations and QM/MM studies etc. were performed to predict the binding mode, to check the stability of the complex and to calculate the interaction energy (Table 4). The study revealed that the interaction of any ligand with the DNA not only depends upon the chemical structure of ligand but also on the DNA sequence. An intercalator intercalates between the base pairs of DNA, if and only if, the DNA has a required intercalation gap between DNA base pairs, otherwise, the ligand will bind to DNA groove (major or minor). Molecular Docking from AUTODOCK shows that if the DNA has intercalation site then minor groove binders are also able to bind as intercalators. MD simulations were performed to check the stability of docked complexes and RMSD analysis confirms that the minor groove binders bind as an intercalator with DNA having intercalation gap that are not stable up to the end of simulation. From the RMSD analysis, the average RMSD variation of minor groove binders that bind to the minor groove of DNA having intercalation site, is always greater than that of the DNA without intercalation site as minor groove binder. So, it is clear from above discussion that on the basis of Molecular Docking only, the exact mode of binding of ligand to DNA cannot be predicted and MD simulation is required to check the stability of docked complexes.

Chapter 7: General Conclusions

The work done in this thesis highlights following general conclusions:

A. The focus of this study is to confirm the importance of DNA sequence and specificity in directing the complex formation at molecular level. Thus, our study attempts to give detailed insight on the complexity in binding modes of small molecules to DNA.

B. In this study, the drug molecules which targeted DNA have been discussed. The array of available computational approaches and molecular modelling methods are being used for complementing the experimental efforts to improve the existing drugs and also in designing novel drug candidates which can act as good DNA inhibitors.

C. The computational studies between minor groove binders and intercalators with DNA show that DNA intercalators generally bind between the CG regions of nucleic acid via π-π interaction between ligand and nucleic acid bases, while minor groove binders form hydrogen bonds between ligands and the functional groups on the bases are exposed in the grooves via their end groups and also their amide or other linker groups in AT-rich region of DNA.

D. The interaction of any ligand to the DNA depends not only on the chemical structure of ligand but also on the DNA sequence. Intercalation requires conformational changes in DNA and a minor groove binder can also as an intercalator if DNA has required intercalation gap and an intercalator bind as minor groove binder if DNA has no intercalation gap.

E. QM/MM calculations provide much better results than that of other molecular modelling methods such as molecular docking and molecular dynamics results. So, QM/MM study provides better insight on the complexity in binding modes of small molecules to DNA. The use of MD simulations approach with QM/MM calculations provides a theoretical protocol for complementing experimental techniques.